

The analysis of inclined anchor plates

R.K. ROWE

Faculty of Engineering Science, University of Western Ontario, London, Canada

J.R. BOOKER

Department of Civil Engineering, University of Sydney, Australia

1 INTRODUCTION

The problem of predicting the behaviour of horizontal anchor plates at working loads has previously been considered for square and rectangular anchors in an incompressible half-space (Fox, 1948) and for circular, rectangular and strip anchors in an elastic layer of finite depth (Rowe and Booker, 1978; Rowe, 1978). Approximate attempts have also been made to predict the behaviour of vertical anchors in an elastic half-space (Douglas and Davis, 1964). However, no consideration appears to have been given to the general effect of anchor inclination upon the elastic behaviour of anchor plates. In this paper, an analytical technique will be presented for the analysis of an anchor of general shape inclined at an angle θ to the horizontal and buried at a depth h below the surface of a homogeneous, isotropic elastic half-space (with elastic modulus E and Poisson's ratio ν) as shown in Fig.1. The anchor plate itself may be either perfectly flexible or rigid and the applied load may be at any point along the anchor and at any inclination to the anchor plate. If desired, the approach may be used to obtain a general load and moment versus displacement and rotation relationship for a particular anchor.

The proposed method of analysis bears some similarity to the boundary integral approach but there are significant differences. The most important of these is the mode of calculation of coefficients for an interaction matrix (relating forces and deflections) and the incorporation of the horizontal free surface. In this paper the anchor is divided into a series of subregions or elements and it is assumed that the forces acting over each subregion can be taken to be uniformly distributed over that sub-region. Deflections are

considered to be composed of two parts; the first corresponds to an infinitely deep anchor and is given analytically for rectangular subregions. The second is expressed as a rapidly convergent Fourier integral and accounts for the presence of the horizontal free surface. Thus in the proposed method, there is no necessity to introduce elements along the stress free surface as there would be in the boundary integral approach.

Once the interaction matrix has been determined it can be used to calculate the force distribution developed when the anchor undergoes a prescribed rigid body movement, or alternatively, to calculate the rigid body movement induced by a prescribed applied resultant force.

2 THEORY

In Fig.1 R is a thin rigid anchor plate embedded in a homogeneous isotropic half-space. When the anchor is loaded it will exert tractions on the surrounding elastic material. In order to analyse the behaviour of the anchor plate suppose that the region R is divided into n subregions or elements R_i as indicated in Fig.1; suppose further that, to sufficient accuracy, the net traction acting on R_i can be assumed to be uniformly distributed. Let \bar{w}_j denote the average deflection of the j th subregion, then it follows from the theory of elasticity that \bar{w}_j can be expressed in the form

$$\bar{w}_j = \sum_{k=1}^n I_{jk} P_k \quad (1)$$

where I_{jk} is a 3 x 3 matrix of influence coefficients to be determined in the next section

and P_k is net force acting on element k .

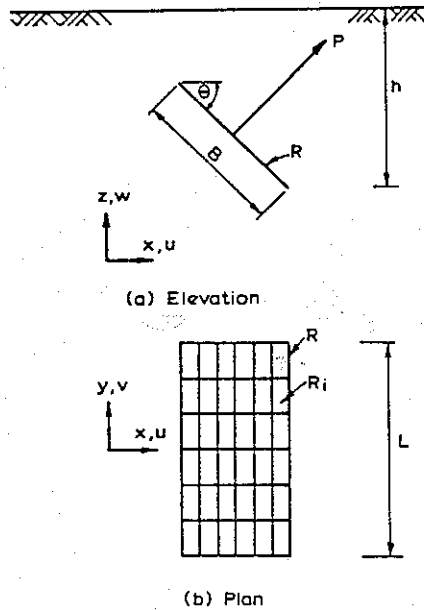


Fig.1 Typical problem configuration

Equation (1) may also be written in the matrix form

$$\underline{D} = \underline{J} \underline{F} \quad (2)$$

where $\underline{D}^T = (\bar{w}_1^T, \dots, \bar{w}_n^T)$ is the vector of element deflections

$\underline{F}^T = (p_1^T, \dots, p_n^T)$ is the vector of element forces

\underline{J} is the $3n \times 3n$ partitioned matrix

$$\underline{J} = \begin{bmatrix} \underline{I}_{11} & \dots & \underline{I}_{1n} \\ \vdots & \ddots & \vdots \\ \underline{I}_{n1} & \dots & \underline{I}_{nn} \end{bmatrix} \quad (3)$$

The deflection of the plate may be expressed in the form

$$\bar{w}_i = A_i \underline{R} \quad (4)$$

where $\underline{R} = (w_{x_0}, w_{y_0}, w_{z_0}, \theta_x, \theta_y, \theta_z)^T$

is the vector of rigid body movements

$$\text{and } A_i = \begin{bmatrix} 1, 0, 0, & 0, & -(\bar{z}_i - z_0), & +(\bar{y}_i - y_0) \\ 0, 1, 0, & +(\bar{z}_i - z_0), & 0, & -(\bar{x}_i - x_0) \\ 0, 0, 1, & -(\bar{y}_i - y_0), & +(\bar{x}_i - x_0), & 0 \end{bmatrix}$$

and $\bar{x}_i, \bar{y}_i, \bar{z}_i$ are the coordinates of the centroid of R_i

The forces p_i and moments m_i exerted on each element are given by

$$\begin{bmatrix} p_i \\ m_i \end{bmatrix} = A_i^T \underline{P}_i \quad (5)$$

The overall equilibrium of body may, therefore, be expressed

$$\underline{K} = \underline{B}^T \underline{F} \quad (6)$$

where $\underline{K}^T = (\underline{T}^T, \underline{O}^T)$ is the vector of applied forces and moments

and \underline{B}^T is $6 \times 3n$ partitioned matrix

$$\underline{B}^T = (A_1^T, \dots, A_n^T)$$

Combining equations (2, 4, 6) it is found that

$$\begin{bmatrix} \underline{J}, \underline{B} \\ -\underline{B}^T, \underline{O} \end{bmatrix} \begin{bmatrix} \underline{F} \\ \underline{R} \end{bmatrix} = \begin{bmatrix} \underline{O} \\ -\underline{K} \end{bmatrix} \quad (7)$$

a set of $3n+6$ equations in the $3n+6$ unknowns $\underline{P}_i, \underline{R}$.

2.1 Determination of influence matrices

The influence coefficients in equation (1) can be obtained by integrating Mindlin's equations, Mindlin (1936), for source points ranging over R_k and field points ranging over R_i . Certain of these integrals can be evaluated analytically for vertical and horizontal anchors (Davis and Douglas (1964), Chapman and Groth (1969)). However it does not appear possible to perform the integrations analytically in the general case.

It is therefore necessary to adopt an alternative approach. The equations of elasticity are transformed by the application of a double Fourier transform, Sneddon (1951), or equivalently the displacements are assumed to have the Fourier representation

$$w(x, y, z) = \int_{-\infty}^{\infty} \int_{-\infty}^{\infty} e^{i(\alpha x + \beta y)} W(\alpha, \beta, z) d\alpha d\beta \quad (8)$$

Suppose the half space is bounded by the plane $z = z_b$, it is required to find the displacements at the field point (x_f, y_f, z_f) due to a point load of intensity located at the source point (x_s, y_s, z_s) .

It is convenient to break the solution into two parts

$$\underline{w} = \underline{w}_k + \underline{w}_c \quad (9)$$

where \underline{w}_k is the deflection due to a point load in a complete space, Kelvin solution, $z_b \rightarrow -\infty$

and \underline{w}_c is the correction to the Kelvin solution

Clearly the correction solution is the solution for a half space, $z \geq z_b$, subjected to surface tractions equal in magnitude but opposite in sign to those generated by the Kelvin solution. It is then not difficult to establish that

$$\underline{w}_c = \frac{H^T N^T(z_b - z_f) \Delta N(z_b - z_s)}{8\pi(1+\psi) \psi G \rho} H \underline{P} \quad (10)$$

$$\text{where } \underline{P} = \underline{P} \frac{e^{-i(\alpha x_s + \beta y_s)}}{4\pi^2}$$

$$\lambda = \frac{E \nu}{(1+\nu)(1-2\nu)}, \quad G = \frac{E}{2(1+\nu)} \quad \text{are Lamé's parameters}$$

$$\psi = \frac{\lambda + G}{\lambda + 3G}$$

$$\rho = \sqrt{\alpha^2 + \beta^2}$$

$$H = \begin{bmatrix} \alpha/\rho & \beta/\rho & 0 \\ -\beta/\rho & \alpha/\rho & 0 \\ 0 & 0 & 1 \end{bmatrix}$$

$$\Delta = \text{diag. } (1, 4\psi(1+\psi), 1)$$

$$\text{and } N(z) = e^{-\rho z} \begin{bmatrix} 1+\psi+2\psi\rho z & 0, +i(1-\psi-2\psi\rho z) \\ 0 & 1, 0 \\ -i(1-\psi)+2\psi\rho z, 0, 1+\psi-2\psi\rho z \end{bmatrix}$$

and thus that

$$\underline{w}_c = \left[\int_{-\infty}^{\infty} \int_{-\infty}^{\infty} \frac{Q_{bf}^T \Delta Q_{bs}}{32\pi^2(1+\psi)\psi G \rho} d\alpha d\beta \right] \underline{P} \quad (11)$$

$$\text{where } Q_{bf} = Q(x_f, y_f, z_b - z_f)$$

$$Q_{bs} = Q(x_s, y_s, z_b - z_s)$$

$$\text{and } Q(x, y, z) = e^{-i(\alpha x + \beta y)} N(z) H$$

Returning to equation (9) it can be seen that the influence matrix I_{jk} can be broken into two parts

$$I_{jk} = L_{jk} + M_{jk} \quad (12)$$

the first L_{jk} arises from the Kelvin solution and is evaluated analytically for rectangular elements in the appendix, the second arises from the correction terms and is evaluated by integrating equation (11)

$$M_{jk} = \int_{-\infty}^{\infty} \int_{-\infty}^{\infty} \frac{\Omega_j^T \Delta \Omega_k}{32\pi^2 G(1+\psi)\psi \rho} d\alpha d\beta \quad (13)$$

$$\text{where } \Omega_k = \frac{1}{A_k} \iint Q(x_s, y_s, z_b - z_s) dS_s$$

$$= \frac{1}{A_k} \iint Q(x_f, y_f, z_b - z_f) dS_f$$

and A_k is the area of the element R_k .

The integration indicated by equation (13) can be performed analytically for rectangular elements. The evaluation of the influence matrix M_{jk} in equation (12) can be simplified by introducing polar coordinates

$$\alpha = \rho \cos \epsilon \\ \beta = \rho \sin \epsilon \quad (14)$$

so that

$$M_{jk} = \int_0^{\infty} \left(\int_0^{2\pi} \frac{\Omega_j^T \Delta \Omega_k d\epsilon}{32\pi^2 G(1+\psi)\psi} \right) d\rho \quad (15)$$

this integral may then be evaluated numerically using Gaussian quadrature. The integral converges rapidly and generally only requires one integration step in both the ϵ and ρ directions. It is usually sufficient to use eight sample points and to integrate with respect to ρ between the limit of zero and 10B. However higher accuracy is required for very shallow anchors.

3 THE EFFECT OF INCLINATION UPON ANCHOR BEHAVIOUR

The method of analysis presented in the previous section may be utilised to determine the elastic behaviour of an anchor of general shape. However, for purposes of illustration, attention will be restricted here to the load displacement relationship for a square anchor, expressed in terms of the apparent stiffness $P/B\delta E$, where P is the applied load necessary to cause an anchor of breadth B to displace a distance δ in the direction of the load P (i.e. δ is the displacement of an inextensible anchor rod due to the application of the load P to

the anchor rod). It is further assumed that the anchor is rough and is fully bonded to the soil, since it is generally accepted (e.g. Douglas and Davis, 1964; Selvadurai, 1976; Rowe and Booker, 1978) that this case corresponds to the most practical limiting case for the application of elastic solutions. Unless otherwise stated, analyses were performed for a load applied at the centre of the anchor.

The application of the analytical technique described in section 2 to the prediction of the load displacement behaviour of a rigid anchor plate involves an approximation regarding the number of subregions necessary to simulate rigid anchor behaviour. In this regard it was found that for an anchor at infinite depth, the discrepancy between the apparent stiffness of an anchor subdivided into 4, 16, 36, 64 and 100 subregions and the analytical solution for a circular anchor of equivalent area (Selvadurai, 1976) was 6.3%, 2.5%, 1.2%, 0.4% and .01% respectively for both $\nu = 0.3$ and $\nu = 0.5$. More importantly, however, it was found that for a given number of subdivisions, the ratio, I_h , of the apparent stiffness at any embedment ratio (h/B) to that obtained at infinite depth was largely independent of the number of subdivisions for sixteen or more subdivisions. Even for one subdivision the ratios agreed with that obtained for a rigid anchor to better than 1.5% for embedment ratios greater than or equal to one. It follows, that for many applications it would be sufficiently accurate to perform an analysis using only one subdivision and that in general, no more than 16 subdivisions would be required provided more accurate spot checks are made to ensure that the required accuracy is achieved.

The effects of embedment ratio, Poisson's ratio and anchor inclination can be conveniently represented by expressing the apparent stiffness $P/B\delta E$ in the form

$$\frac{P}{B\delta E} = I_{\infty} \cdot I_h \quad (15)$$

where I_{∞} is an influence factor for the effect of anchor shape and Poisson's ratio, ν , upon the apparent stiffness of an anchor at infinite depth ($h/B=\infty$). I_{∞} is independent of anchor orientation θ .

I_h is a correction factor for the effect of embedment ratio h/B and anchor inclination θ upon the apparent stiffness.

B is the breadth (or diameter, for a circle) of the anchor; and $P, \delta,$ and E are as previously defined.

It has been found that the authors' value of I_{∞} obtained for a rigid square anchor is in excellent agreement with the analytical solution obtained by Selvadurai (1976) for a rigid circular anchor in an infinite soil mass, provided both anchors have the same cross-sectional area. This finding accords with a suggestion by Davis and Poulos (1972) that the settlement of a square surface footing is very little different from that of a circle of equal area.

Thus Selvadurai's general solution for a circle

$$I_{\infty} \text{ (circle)} = \frac{8(1-\nu)}{(1+\nu)(3-4\nu)}$$

may be modified for a square, viz.

$$I_{\infty} \text{ (square)} = \frac{2}{\sqrt{\pi}} \frac{8(1-\nu)}{(1+\nu)(3-4\nu)}$$

Strictly speaking, the solutions obtained in this paper only apply for a square anchor. However since the apparent stiffness of square anchors in the limiting cases (i.e. at the surface and infinitely deep) are almost the same as for circular anchors provided the appropriate value of I_{∞} is selected.

The correction factor I_h is shown in Figs. 2 and 3 as a function of embedment ratio h/B for a range of anchor orientations θ . This correction factor I_h corresponds to the ratio of the apparent stiffness for a given h/B to the apparent stiffness obtained for a similar case where $h/B = \infty$ and consequently, attains a limiting value of unity at the critical embedment ratio. Any increase in embedment beyond the critical value will not alter the apparent stiffness of the anchor. The rate of increase in apparent stiffness with embedment ratio is relatively fast for embedment ratios less than 5 and at an embedment ratio of 5 the apparent stiffness of the anchor is between 91 and 96% of the infinitely deep value. However the rate of increase in stiffness with embedment ratio reduces rapidly for h/B greater than 5 and the apparent stiffness does not attain 99% of the infinitely deep value until an embedment ratio (h/B) of between 20 and 50.

For a given embedment ratio, anchor inclination may alter the apparent stiffness of the anchor by up to 8% with the greatest differences occurring for anchors at moderately shallow depths (i.e. $1.5 < h/B < 4$). However in situations where different anchor orientations are considered, the definition of embedment ratio is somewhat arbitrary. In this paper the depth, h , is the distance from the soil surface to the bottom of the anchor.

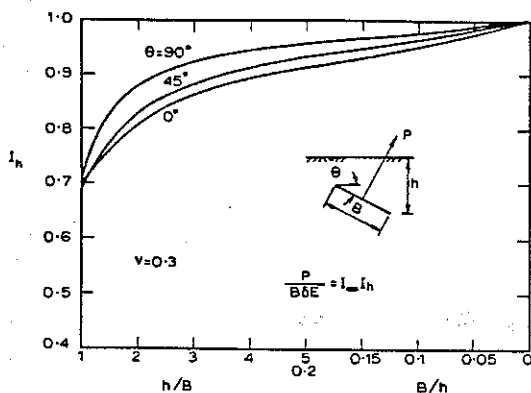


Fig. 2 Correction factor I_h for the effect of embedment upon apparent stiffness $\nu=0.3$

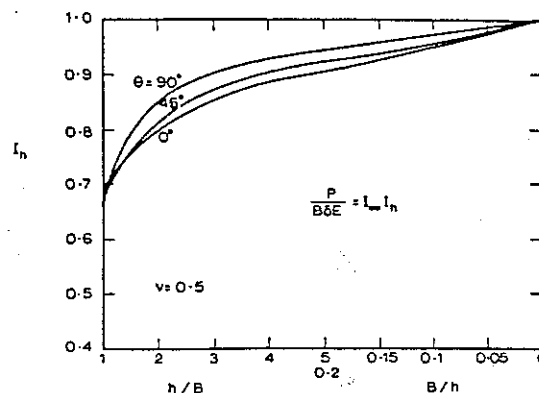


Fig. 3 Correction factor I_h for the effect of embedment ratio upon apparent stiffness $\nu=0.5$

An alternative definition might take the depth, h , as the distance to the top or midpoint of the anchor. In this case the effect of anchor orientation would appear to be much greater although, clearly, the apparent stiffness of the anchor for a particular case is independent of the definition used in the graphical presentation of solutions.

The effect of anchor inclination upon the elastic response of the anchor may be better appreciated from Figs. 4 and 5 which show the correction factor, I_h , as a polar function of anchor inclination θ . The difference in the apparent stiffness of an anchor subjected to a centrally applied point load and that of an anchor subjected to loading which would cause rigid normal displacement without rotation is also illustrated in these figures. The effect is generally small and is insignificant for embedment ratio greater than 2. The magnitude of observed anchor rotations for an anchor subjected to a central point load is shown in Figs. 6 and 7. Here the anchor displacement at the top (δ_t) and bottom (δ_b) of the anchor are given in terms of the displacement at the centre of the anchor (δ). The magnitude of anchor rotation increases with increasing anchor inclination θ and decreasing embedment ratio h/B . In the worst case ($h/B = 1$, $\nu = 0.5$, $\theta = 90^\circ$) the top displacement is almost 17% greater than the central displacement; however the magnitude of anchor rotation decreases rapidly with embedment and even for an embedment ratio of 2 the difference is less than 2.6%.

The foregoing solutions have all been for the case of an applied load perpendicular to the anchor plate. However, the approach given in section 2 may be used to obtain solutions for a wide range of load-

ing conditions. One case of some practical importance is that where the load is applied at some angle α to the normal to the anchor plate as shown in Fig. 8a. In this case the apparent stiffness $P/B\delta E$ may be expressed in the form

$$\frac{P}{B\delta E} = I_\infty I_h I_\alpha$$

where I_α is a correction factor for the effect of load inclination upon the apparent stiffness; and P , B , δ , E , I_∞ , and I_h are as previously defined.

The correction factor I_α is shown in Figs. 8 and 9 for a range of anchor inclinations α . The effect of load inclination α is greatest at shallow depth and for high anchor inclinations θ . The effect decreases rapidly with embedment ratio. It will be noted that at shallow depth the load-deflection response of the anchor may be enhanced for some load inclinations greater than zero; however, in general, inclination of the load tends to reduce the apparent stiffness of the anchor by up to almost 25% over the range of inclination considered. At shallow depths there is a marked interaction between anchor and the inclination of the load to the anchor. As might be expected, at great depth the response of the anchor is independent of anchor inclination although the inclination of the load may still reduce the apparent stiffness significantly.

4 CONCLUSION

An analytical technique has been presented for the prediction of the behaviour of an

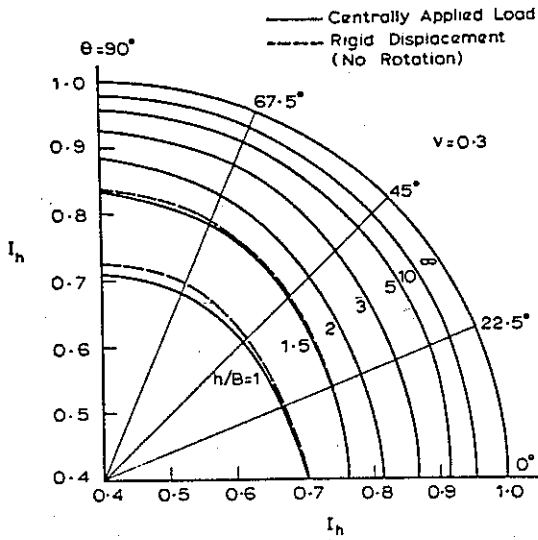


Fig.4 Variation in I_h with anchor inclination θ for $\nu = 0.3$

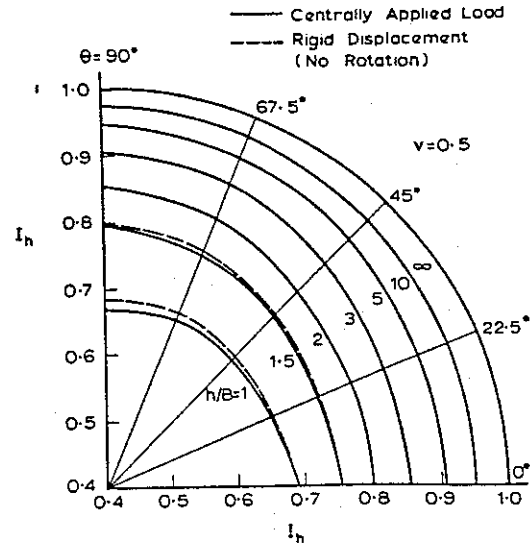


Fig.5 Variation in I_h with anchor inclination θ for $\nu = 0.5$

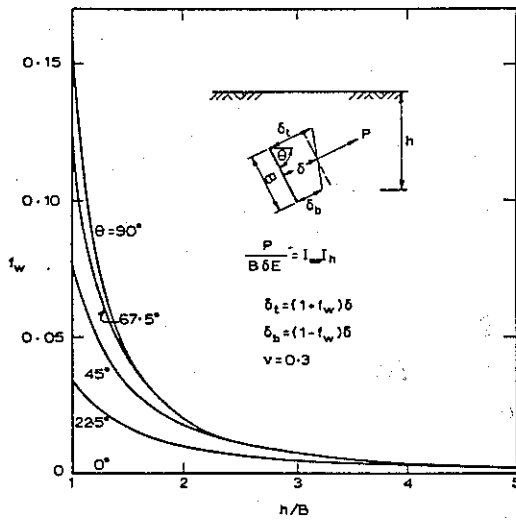


Fig.6 Correction factor f_w for anchor displacement at top and bottom of anchor

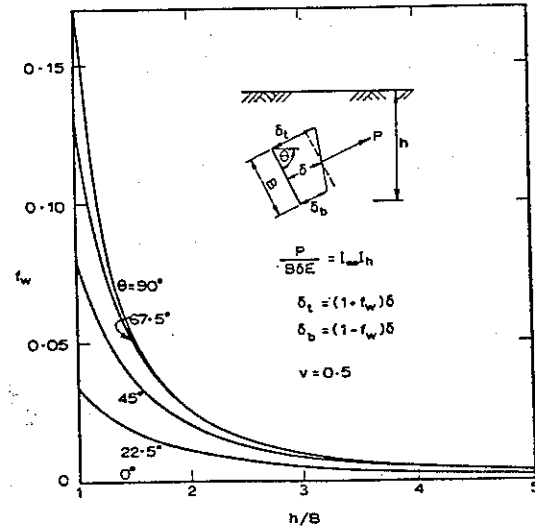


Fig.7 Correction factor f_w for anchor displacement at top and bottom of anchor

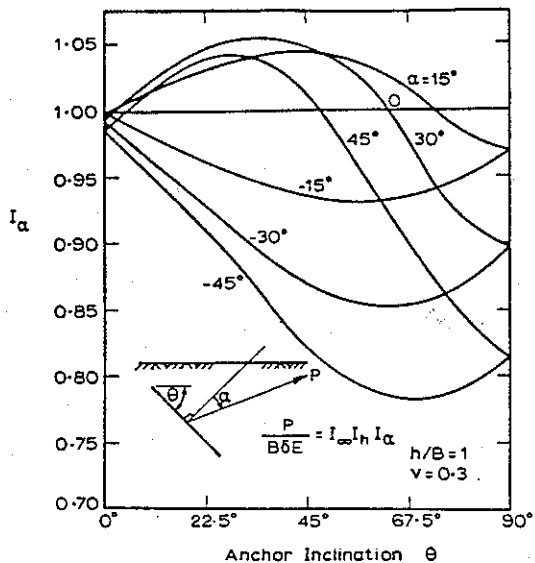


Fig.8a Effect of load inclination α for $v = 0.3$

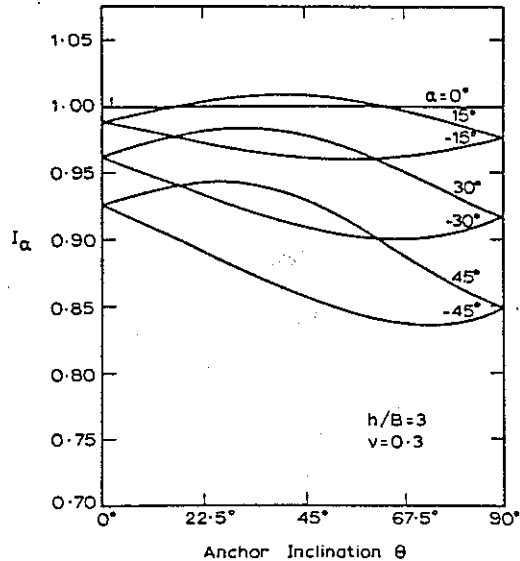


Fig.8b Effect of load inclination α for $v = 0.3$

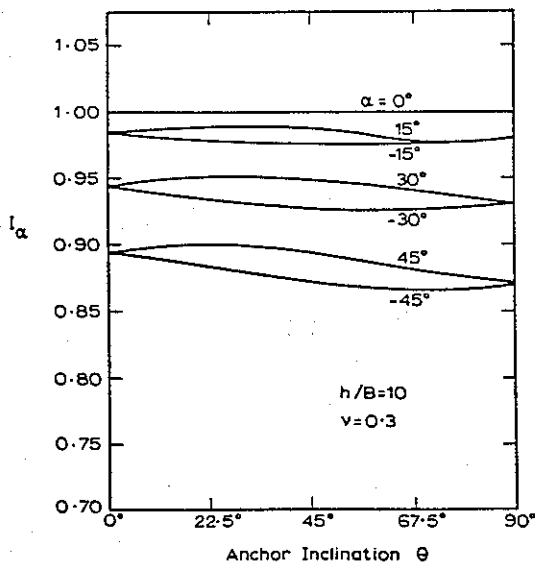


Fig.8c Effect of load inclination α for $v = 0.3$

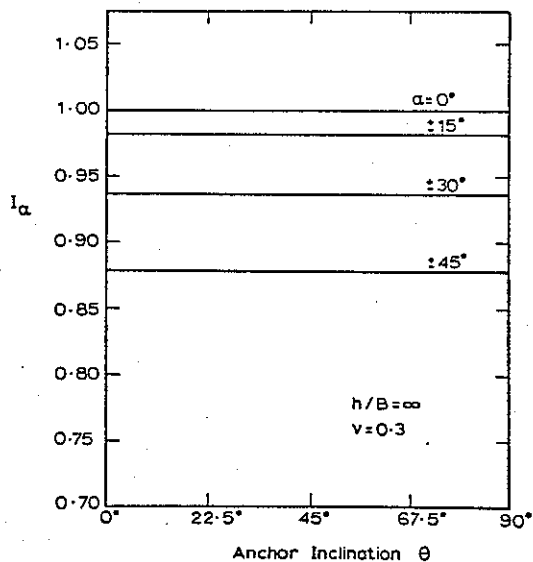


Fig.8d Effect of load inclination α for $v = 0.3$

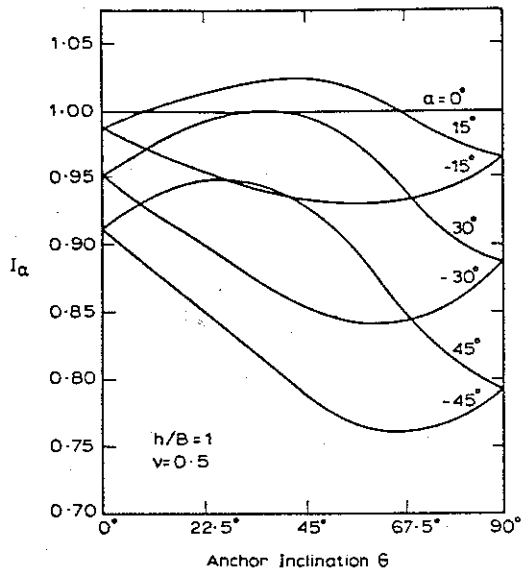


Fig.9a Effect of load inclination α for $\nu = 0.5$

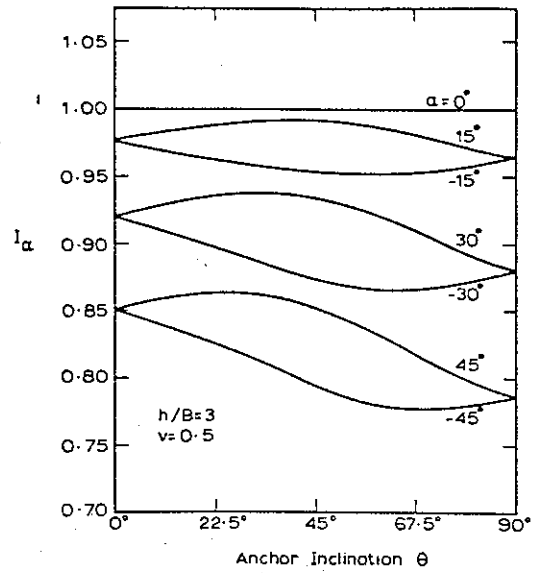


Fig.9b Effect of load inclination α for $\nu = 0.5$

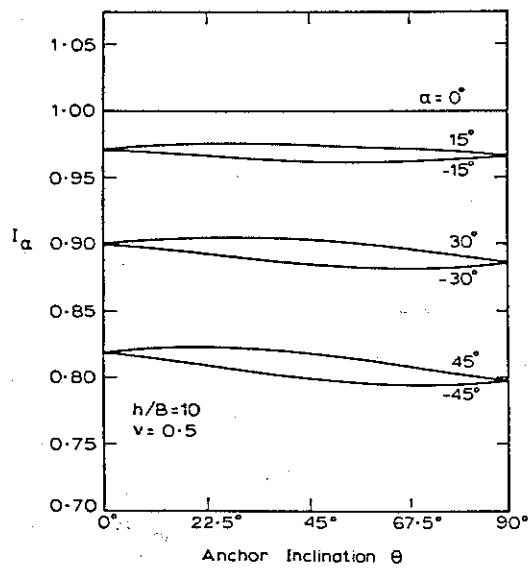


Fig.9c Effect of load inclination α for $\nu = 0.5$

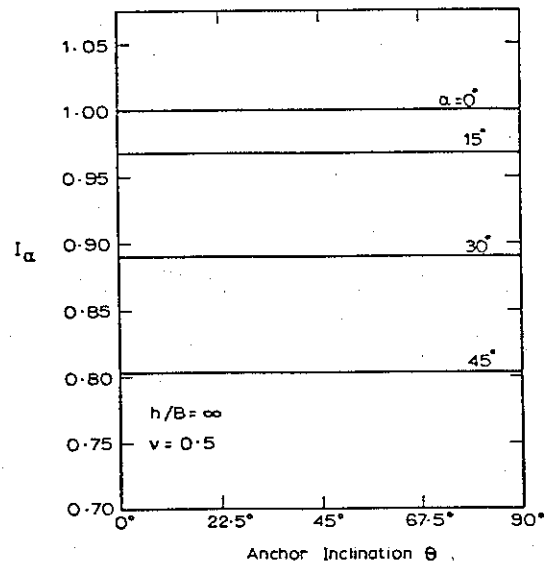


Fig.9d Effect of load inclination α for $\nu = 0.5$

inclined anchor in an elastic soil medium. The anchor may be of general shape but is divided into a series of rectangular sub-regions or elements. The anchor may be subjected to quite general loading conditions.

The approach has been applied to the particular case of a square anchor and solutions are presented for the elastic response of the anchor for a wide range of material and geometric parameters. These solutions are presented in the form of influence charts which may be used directly in hand calculations to predict the elastic load deflection behaviour of anchor plates for a range of Poisson's ratio, embedment ratio anchor inclinations and load inclinations.

It is considered that the solutions presented for the apparent stiffness of a square anchor may be used for circular anchors of equal area.

5 REFERENCES

- Chapman, C.R. and N.N.Groth 1969, Computer evaluation of deformation due to sub-surface loads in a semi-infinite elastic medium, B.E. Thesis, Univ. of Sydney, Aust.
- Davis, E.H. and H.G.Poulos 1972, Rate of settlement under three dimensional conditions, Geotechnique 22, p. 95.
- Douglas, D.J. and E.H. Davis 1964, The movements of buried footings due to moment and horizontal load and the movement of anchor plates, Geotechnique, Vol.14, No.2, pp. 115-132
- Fox, E.N. 1948, The mean elastic settlement of a uniformly loaded area at a depth below the ground surface, Proc. 2nd Inst. Conf. Soil Mech. Fndn Eng., Vol.1, p.129.
- Mindlin, R.D. 1936, Force at a point in the interior of a semi-infinite solid, Jnl. Appl. Phys. Vol. 7, No.5, pp. 195-202.
- Rowe, R.K. 1978, Soil structure interaction analysis and its application to the prediction of anchor plate behaviour, PhD Thesis, Univ. of Sydney, Aust.
- Rowe, R.K. and J.R. Booker 1978, A method of analysis for horizontally embedded anchors in an elastic soil, accepted for publication Int. Jnl. for Num. and Analytical Meth. in Geomechanics; see also School of Civil Engng. Research Report 316, Univ. of Sydney, Aust.
- Selvadurai, A.P.S., 1976, The load-deflection characteristics of a deep rigid anchor in an elastic medium, Geotechnique 26, No.4, pp. 603-612.
- Neddon, I.N. 1951, Fourier transforms, McGraw-Hill, New York.

APPENDIX

The displacement vector w at the field point (x_f, y_f, z_f) corresponding to a point load p applied at the source point (x_s, y_s, z_s) is:

$$\underline{w} = \frac{1}{4\pi G} \left(V \frac{p}{R^{\psi+1}} \begin{bmatrix} R_{xx} & R_{xy} & R_{xz} \\ R_{yx} & R_{yy} & R_{yz} \\ R_{zx} & R_{zy} & R_{zz} \end{bmatrix} p \right) \quad (A1)$$

where $R = (x^2 + y^2 + z^2)^{\frac{1}{2}}$

$$V = I/R$$

$$(x, y, z) = (x_f - x_s, y_f - y_s, z_f - z_s)$$

and the subscripts x, y, z indicate differentiation with respect to that variable.

Let ξ, η, ζ be Cartesian coordinates with ξ, η lying in the plane of the plate. The (x, y, z) and ξ, η, ζ will be related by an orthogonal matrix H as follows

$$\underline{\xi} = H \underline{x} \quad (A2)$$

where $\underline{x} = (x, y, z)^T$

$$\underline{\xi} = (\xi, \eta, \zeta)^T$$

It may be shown that

$$\underline{w} = \frac{1}{4\pi G} \left(V \frac{p}{R^{\psi+1}} H^T \begin{bmatrix} R_{\xi\xi} & R_{\xi\eta} & 0 \\ R_{\eta\xi} & R_{\eta\eta} & 0 \\ 0 & 0 & V \end{bmatrix} H \underline{p} \right) \quad (A3)$$

where $R = (\xi^2 + \eta^2)^{\frac{1}{2}}$

$$V = I/R$$

$$(\xi, \eta) = (\xi_f - \xi_s, \eta_f - \eta_s)$$

and where the subscripts ξ, η indicate differentiation with respect to that variable and the subscripts s, f indicate values at the source and field points respectively.

Next consider two rectangular elements

$$(R_j | a_{jf} \leq \xi_f \leq b_{jf}, c_{jf} \leq \eta_f \leq d_{jf}) \text{ and}$$

$$(R_k | a_{sk} \leq \xi_s \leq b_{sk}, c_{sk} \leq \eta_s \leq d_{sk}) \text{ and let } \chi(\xi, \eta)$$

be a quantity defined over both elements then it can be shown that if χ is any solution of the equation

$$\frac{\partial^4 \chi}{\partial^2 \xi^2 \partial \eta^2} = \phi \quad (A4)$$

then

$$\int_{R_j} \left(\int_{R_k} \phi d\xi_s d\eta_s \right) d\xi_f d\eta_f = \langle X \rangle$$

where

$$\langle X \rangle = \left[\left[\left[\left[X \right]_{a_{sk}}^{b_{sk}} \right]_{c_{sk}}^{d_{sk}} \right]_{a_{fk}}^{b_{fk}} \right]_{c_{fk}}^{d_{fk}}$$

Now let us introduce the notation V^ξ for any solution of the equation

$$\frac{\partial V^\xi}{\partial \xi} = V$$

with similar definitions for V^η etc.

Thus in equation (A4) $X = \phi^{\xi\xi\eta\eta}$

It can now be seen that the matrix I_{jk} is given by

$$I_{jk} = \frac{1}{4\pi G A_j A_k} H^T \left(V^{\xi\xi\eta\eta} I + \begin{bmatrix} R^{\eta\eta} & R^{\xi\eta} & 0 \\ R^{\xi\eta} & R^{\xi\xi} & 0 \\ 0 & 0 & V^{\xi\xi\eta\eta} \end{bmatrix} \right) H \quad (A5)$$

Integration of the functions V, R reveals that

$$V^\xi(\xi, \eta) = \sinh^{-1} \frac{\xi}{|\eta|}$$

$$V^\eta(\xi, \eta) = V^\xi(\eta, \xi) = \sinh^{-1} \frac{\eta}{|\xi|}$$

$$V^{\xi\xi}(\xi, \eta) = \xi V^{\xi-R} \quad (A6)$$

$$V^{\eta\eta}(\xi, \eta) = \eta V^{\eta-R} \quad (A7)$$

$V^{\xi\eta}$ is a homogeneous function of order one thus using Euler's theorem

$$V^{\xi\eta} = \xi V^\eta + \eta V^\xi \quad (A8)$$

Similarly $V^{\xi\xi\eta\eta}$ is a homogeneous function of order 3 and so

$$V^{\xi\xi\eta\eta} = \frac{1}{6} (\xi^2 V^{\eta\eta} + 2\xi\eta V^{\xi\eta} + \eta^2 V^{\xi\xi}) \quad (A9)$$

$$\text{also } R^\xi = \frac{1}{2} (\xi R + \eta^2 V^\xi)$$

$$R^\eta = \frac{1}{2} (\eta R + \xi^2 V^\eta)$$

$$R^{\xi\xi} = \frac{1}{2} \left(\frac{R^3}{3} + \eta^2 V^{\xi\xi} \right) \quad (A11)$$

$$R^{\eta\eta} = \frac{1}{2} \left(\frac{R^3}{3} + \xi^2 V^{\eta\eta} \right) \quad (A12)$$

$R^{\xi\eta}$ is a homogeneous function of order 3 and thus

$$R^{\xi\eta} = \frac{1}{3} (\eta R^\xi + \xi R^\eta) \quad (A13)$$

Equation (A5) can now be evaluated from the results of A6-A13).